AMERICAN ACADEMY™ OF OPHTHALMOLOGY

Clinical and Morphologic Characteristics of MEK Inhibitor–Associated Retinopathy

Differences from Central Serous Chorioretinopathy

Jasmine H. Francis, MD, FACS,[1,2] Larissa A. Habib, MD,[1] David H. Abramson, MD, FACS,[1,2] Lawrence A. Yannuzzi, MD,[3,4] Murk Heinemann, MD,[1,2] Mrinal M. Gounder, MD,[2,6] Rachel N. Grisham, MD,[2,5] Michael A. Postow, MD,[2,6] Alexander N. Shoushtari, MD,[2,6] Ping Chi, MD, PhD,[6,7] Neil H. Segal, MD, PhD,[6] Rona Yaeger, MD,[6] Alan L. Ho, MD, PhD,[2,6] Paul B. Chapman, MD,[2,6] Federica Catalanotti, PhD[1]

Purpose: To investigate the clinical and morphologic characteristics of serous retinal disturbances in patients taking mitogen-activated protein kinase kinase (MEK) inhibitors.

Participants: A total of 313 fluid foci in 50 eyes of 25 patients receiving MEK inhibitors for treatment of their metastatic cancer, who had evidence of serous retinal detachments confirmed by optical coherence tomography (OCT).

Design: Single-center, retrospective cohort study.

Methods: Clinical examination and OCT were used to evaluate MEK inhibitor–associated subretinal fluid. The morphology, distribution, and location of fluid foci were serially evaluated for each eye. Choroidal thickness was measured at each time point (baseline, fluid accumulation, and fluid resolution). Two independent observers performed all measurements. Statistical analysis was used to correlate interobserver findings and compare choroidal thickness and visual acuity at each time point.

Main Outcome Measures: Comparison of OCT characteristics of retinal abnormalities at baseline to fluid accumulation.

Results: The majority of patients had fluid foci that were bilateral (92%) and multifocal (77%) and at least 1 focus involving the fovea (83.3%). All fluid foci occurred between the interdigitation zone and an intact retinal pigment epithelium. The 313 fluid foci were classified into 4 morphologies, as follows: 231 (73.8%) dome, 36 (11.5%) caterpillar, 31 (9.9%) wavy, and 15 (4.8%) splitting. Best-corrected visual acuity at fluid resolution was not statistically different from baseline; and no eye lost more than 2 Snellen lines from baseline at the time of fluid accumulation. There was no statistical difference in the choroidal thickness between the different time points (baseline, fluid accumulation, and fluid resolution). A strong positive interobserver correlation was obtained for choroidal thickness measurements ($r = 0.97$, $P < 0.0001$) and grading of foci morphology ($r = 0.97$, $P < 0.0001$).

Conclusion: The subretinal fluid foci associated with MEK inhibitors have unique clinical and morphologic characteristics, which can be distinguished from the findings of central serous chorioretinopathy. In this series, MEK inhibitors did not cause irreversible loss of vision or serious eye damage. *Ophthalmology 2017;124:1788-1798 © 2017 by the American Academy of Ophthalmology*

Supplemental material available at www.aaojournal.org.

Human cancers commonly have dysregulation of the mitogen-activated protein kinase (MAPK), and may be amenable to treatment with targeted agents that block this pathway, such as mitogen-activated protein kinase kinase (MEK) inhibitors.[1–4] Targeted agents have a different toxicity profile compared with traditional chemotherapy.[5] Specifically, MEK inhibitors have been associated with self-limited serous detachments of the neurosensory retina, which have been designated MEK inhibitor–associated retinopathy (MEKAR).[6–12]

Some groups and authors have labeled these neurosensory detachments with the description of "central serous retinopathy (CSR)" or "CSR-like."[11,13–15] A recent editorial has suggested MEKAR is intriguing owing to "its similarity to central serous chorioretinopathy" and its potential to deepen our understanding of this latter visually-threatening disease.[16] The authors of this published editorial dedicate a paragraph to discussing the differences between MEKAR and central serous chorioretinopathy (CSC), and others have also commented on these distinctions.[9,10,16]

© 2017 by the American Academy of Ophthalmology
Published by Elsevier Inc.
http://dx.doi.org/10.1016/j.ophtha.2017.05.038
ISSN 0161-6420/17

However, the discussion of these differences is limited to a few points: the "presentation and location" of the fluid are distinct and retinal pigment epithelial detachments (PEDs) and fluorescein leakage are absent in MEKAR. In some reports, there is no further elaboration on these statements, or the assertion is based on fewer than a handful of patients or simply represents a citation of another paper.

In an effort to better understand this topic, this study systematically explored additional characteristics that may differ between these 2 disease entities (MEKAR and CSC). By carefully evaluating over 300 fluid foci in eyes of cancer patients on MEK inhibition, this study analyzed the clinical and morphologic characteristics and the associated retinal, retinal pigment epithelium (RPE), and choroidal changes. Through this analysis, the differences between MEKAR and CSR are discussed: known findings are confirmed and new findings are described.

Methods

The study adhered to the tenets of the Declaration of Helsinki and was approved by the Institutional Review Board of Memorial Sloan Kettering Cancer Center. This retrospective, single-center study included 25 patients recruited from Memorial Sloan Kettering Cancer Center, New York, New York, between October 2012 and February 2017. Patients were enrolled in a prospective MEK inhibitor study for treatment of their metastatic cancer and exhibited subretinal fluid on optical coherence tomography in 1 or both eyes.

Examination

All enrolled patients received an ophthalmologic examination complete with best-corrected visual acuity (BCVA), automated refraction, intraocular pressure, dilated fundus examination, and fundus photography. Enhanced-depth imaging optical coherence tomography (OCT) images were obtained with the Heidelberg Spectralis HRA+OCT (Heidelberg Engineering). A scan of 9 mm was used and a 32-line cross-scan patterns were chosen in the horizontal direction, consisting of a maximum of 50 averaged scans. Patients were examined at baseline, followed by examinations either required by the study protocol (in all but 1 protocol) or conducted if the patient was symptomatic. All but 1 patient was on a protocol that required scheduled examinations irrespective of symptoms (Table S1, available at www.aaojournal.org).

Data Collection

Demographic data were collected on each patient, including gender, age, and primary cancer diagnosis. Treatment data included the initial drug, dose, route, frequency, duration, number of cycles, concomitant drugs, and any alterations in this plan over the treatment course. Clinical data included best-corrected visual acuity (in Snellen and logMAR) at baseline, fluid accumulation and fluid resolution, and whether the patient was symptomatic at the time of fluid accumulation. Further data included time from medication start to initial subretinal fluid detection by OCT, the cycle number during which subretinal fluid was initially detected by OCT, and time to resolution of subretinal fluid by OCT (evaluable in 39 eyes: for 5 patients [10 eyes] there were no adequate images available at the time of fluid resolution and 1 eye developed no serous detachment).

By OCT, the foci of fluid were carefully examined for each eye: details on the number of foci, laterality of foci, location within the fundus, location within OCT layers, configuration/morphology of fluid, caliber of the OCT layers, and other chorioretinal abnormalities (intraretinal cysts, presence of PED, hyperreflective dots) were all recorded. Two independent observers performed grading of the fluid foci morphology and an interobserver correlation was calculated.

Choroidal thickness was measured on enhanced-depth imaging OCT with the caliper tool, as the vertical distance from the hyperreflective line (corresponding to the Bruch membrane) to the chorioscleral border. Two independent observers performed manual segmentation of the choroid at all measurement points, and the mean of both measurements was used for analysis. Choroidal thickness was measured in the location corresponding to the focus of subfoveal subretinal fluid and was evaluable for 32 eyes. In 2 eyes with nonfoveal foci, a location corresponding with an adjacent fluid focus was measured. Choroidal thickness was compared from baseline to fluid accumulation (evaluable in 32 eyes), fluid accumulation to resolution (evaluable in 31 eyes), and baseline to fluid resolution (evaluable in 29 eyes). Eyes were deemed inevaluable if no images were available or if the OCT image was not enhanced-depth, which is preferred for assessment of choroidal thickness.

Statistical Analysis

Choroidal thickness was expressed as mean ± standard error of the mean. Interobserver correlation for all measurements was determined using Pearson correlation. The mean choroidal thickness measurements, and grading of fluid foci morphologies, between observer 1 and observer 2 were used for comparison and statistical analysis. Choroidal thickness was analyzed with a paired 2-tailed t test and confirmed with a 2-way analysis of variance. A P value less than or equal to 0.05 was considered statistically significant. Statistical analysis was performed using GraphPad software (GraphPad Software, Inc, La Jolla, CA).

Results

Fifty eyes of 25 patients with MEK inhibitor–associated subretinal fluid were evaluated. Details regarding patient characteristics and drug information are provided in Table 1. Primary cancer diagnoses included cutaneous melanoma, ovarian cancer, gastrointestinal stromal tumor, colon cancer, uveal melanoma (1 patient; included fellow eye), and thyroid cancer. The mean patient age was 59 years (median, 61 years; range, 22–81 years). Seventeen of 25 patients (68%) were female.

The median duration of the first cycle was 1 day (range, 1–7 days) and the median frequency of the cycles was 4 weeks (range, 3–5 weeks). The median time from medication start to initial subretinal fluid detection by OCT was 14 days (mean, 28.0 days). The abnormal OCT findings were found after a median of 1 cycle of drug (mean, 1.4 cycles of drug, range, 1–4 cycles): 80% of patients had abnormal OCT findings after a single cycle of drug. The overall median time to resolution of the subretinal fluid by OCT was 32 days (mean, 47.4 days; range, 5–182 days). Of evaluable eyes receiving 5 cycles or less, the median time to resolution was 21 days (mean, 35 days, n = 24 eyes). Of evaluable eyes receiving more than 5 cycles, the median time to resolution was 54 days (mean, 65.1 days; n = 15 eyes). In all cases of bilateral fluid foci, resolution occurred at the same time for both eyes. In all eyes, the fluid was self-limiting and did not require discontinuation of the drug.

Concomitant drugs in 7 of the protocols included panitumumab, dabrafenib, ribociclib, imatinib, atezolizumab, encorafenib, and buparlisib. There was no difference in the mean number of foci

Table 1. Patient Characteristics and Drug Information for Study Patients

Pt	Age (Yrs)	Primary Cancer Diagnosis	Drug	Int Dose	Int Drug Freq	Int Dur Cycle (Days)	Int Cycle Freq	Total # Cycles	Change in Dose	Symptoms*
1	65.2	Colorectal cancer	Binimetinib	45 mg	bid	1	q4wks	3	No	No
2	63.0	Cutaneous melanoma	Trametinib	2 mg	daily	1	q4wks	4	No	Yes (1)
3	44.8	Cutaneous melanoma	Binimetinib	45 mg	bid	1	q4wks	8	Yes	No
4	69.1	Cutaneous melanoma	Binimetinib	45 mg	bid	1	q4wks	1	No	Yes (1, 4)
5	21.7	Cutaneous melanoma	Binimetinib	45 mg	bid	7	q3wks	2	No	No
6	69.9	GIST	Binimetinib	45 mg	bid	1	q4wks	4	Yes	No
7	71.6	GIST	Binimetinib	30 mg	bid	7	q4wks	11	No	Yes (1)
8	58.1	GIST	Binimetinib	30 mg	bid	7	q4wks	1	No	No
9	48.5	Colorectal cancer	Cobimetinib	60 mg	daily	7	q4wks	3	Yes	Yes (1)
10	68.7	Colorectal cancer	Cobimetinib	60 mg	daily	7	q4wks	6	No	Yes (1, 3)
11	41.0	Colorectal cancer	Binimetinib	45 mg	bid	7	q4wks	2	No	No
12	47.5	Ovarian cancer	Binimetinib	45 mg	bid	1	q4wks	12	Yes	Yes (3, 4)
13	81.4	Cutaneous melanoma	Binimetinib	45 mg	bid	7	q4wks	10	No	Yes (1)
14	57.9	Ovarian cancer	Binimetinib	45 mg	bid	1	q4wks	2	No	Yes (1)
15	61.1	Uveal melanoma	Trametinib	2 mg	daily	7	q4wks	3	No	No
16	54.1	Cutaneous melanoma	Binimetinib	45 mg	bid	7	q3wks	4	Yes	No
17	53.5	Ovarian cancer	Binimetinib	45 mg	bid	1	q4wks	3	No	Yes (1)
18	57.3	Cutaneous melanoma	Binimetinib	45 mg	bid	1	q4wks	14	Yes	No
19	64.3	Ovarian cancer	Binimetinib	45 mg	bid	1	q4wks	20	Yes	Yes (1)
20	61.4	Ovarian cancer	Binimetinib	45 mg	bid	1	q4wks	8	Yes	Yes (1, 2)
21	54.9	GIST	Binimetinib	30 mg	bid	7	q4wks	17	Yes	No
22	66.9	Ovarian cancer	Binimetinib	45 mg	bid	1	q5wks	2	No	No
23	53.2	Thyroid carcinoma	Selumetinib	75 mg	bid	1	q3wks	2	No	No
24	61.4	Ovarian cancer	Binimetinib	45 mg	bid	1	q4wks	26	Yes	No
25	70.4	Ovarian cancer	Binimetinib	45 mg	bid	1	q4wks	2	No	Yes (2, 4)

Bid = twice a day; Dur = duration; Freq = frequency; GIST = gastrointestinal stromal tumor; Int = initial; Pt = patient; q = every.
*1 = blurry vision; 2 = metamorphopsia; 3 = seeing bubbles/doughnuts; 4 = orange glow.

between eyes in patients treated with monotherapy and those treated with combination treatment (6.4 vs. 6.0, $P = 0.85$).

Clinical Characteristics of the Subretinal Fluid

Details on the location and number of fluid foci per eye are schematically outlined in Figure 1. The foci of fluid appeared as yellow-gray elevations of the fundus, either in a circular shape or in the configuration of nongravitational globules without inferior fluid tracking (similar in shape to mercury beads). Twenty-three of 25 patients (92%) had subretinal fluid in both eyes. In the 2 patients with unilateral subretinal fluid, the fellow eye had a history of retinal detachment: 1 from a rhegamatogenous detachment and the other from uveal melanoma and treatment by plaque brachytherapy. These 2 eyes had retinal atrophy and intraretinal cysts with an intact retinal pigment epithelium but no clear presence of an interdigitation zone (IZ) or ellipsoid zone (EZ).

Thirty-seven of 48 eyes with fluid (77%) had multiple foci of subretinal fluid. Of the 7 patients (11 eyes) with unifocal fluid, 5 patients had unifocal fluid in both eyes. In 40 of 48 eyes (83.3%), at least 1 of the foci of subretinal fluid involved the fovea. The median number of fluid foci per eye was 6 (mean, 6.5; range, 1−21). Note that the location and number of foci was relatively symmetrical between both eyes.

Visual Acuity

Twelve patients (48%) reported symptoms at the time of fluid accumulation. Twelve of 21 (57.1%) patients with fovea foci in at least 1 eye had symptoms, in contrast to 0 of 4 patients without fovea foci in either eye; this was not statistically different ($P = 0.1$). In all evaluable eyes, the BCVA ranged between 20/20 and 20/40 at baseline, from 20/20 to 20/50 at fluid accumulation, and from 20/20 to 20/40 at fluid resolution. The Snellen BCVA lines for all eyes from baseline to fluid accumulation and baseline to fluid resolution are depicted in Figure 2. No eye lost more than 2 lines of Snellen vision from baseline to fluid accumulation. At time of fluid resolution, no eye was less than 1 Snellen line from its baseline vision. The mean and median logMAR BCVA was as follows: at baseline 0.06 and 0, at fluid accumulation 0.1 and 0.1, and at fluid resolution 0.06 and 0. The logMAR BCVA at fluid accumulation was significantly worse than baseline ($P = 0.03$), but logMAR BCVA at fluid resolution was not significantly different from baseline ($P = 0.97$).

Optical Coherence Tomography Characteristics of the Subretinal Fluid

The OCT morphology of the subretinal fluid could be divided into 4 types, as depicted in Figures 1 and 3. The grading of these morphologies had a strong positive interobserver correlation ($r = 0.97$, $P < 0.0001$). Dome (Fig 3, upper left) refers to dome-shaped fluid accumulation between the IZ and RPE akin to the configuration that is observed in classic central serous chorioretinopathy. Small dome foci may only displace the outer retinal layers inward toward the vitreous, whereas larger dome foci displace both the outer and inner retinal layers. Caterpillar (Fig 3, upper middle) refers to a straight or plateau, low-lying accumulation of fluid, which displaces a portion of the IZ (and outer retinal layers) inward toward the vitreous. Wavy (Fig 3, upper right) refers to a linear collection of tiny dome-shaped fluid collections, which displace the IZ (and outer retinal layers) in an undulating,

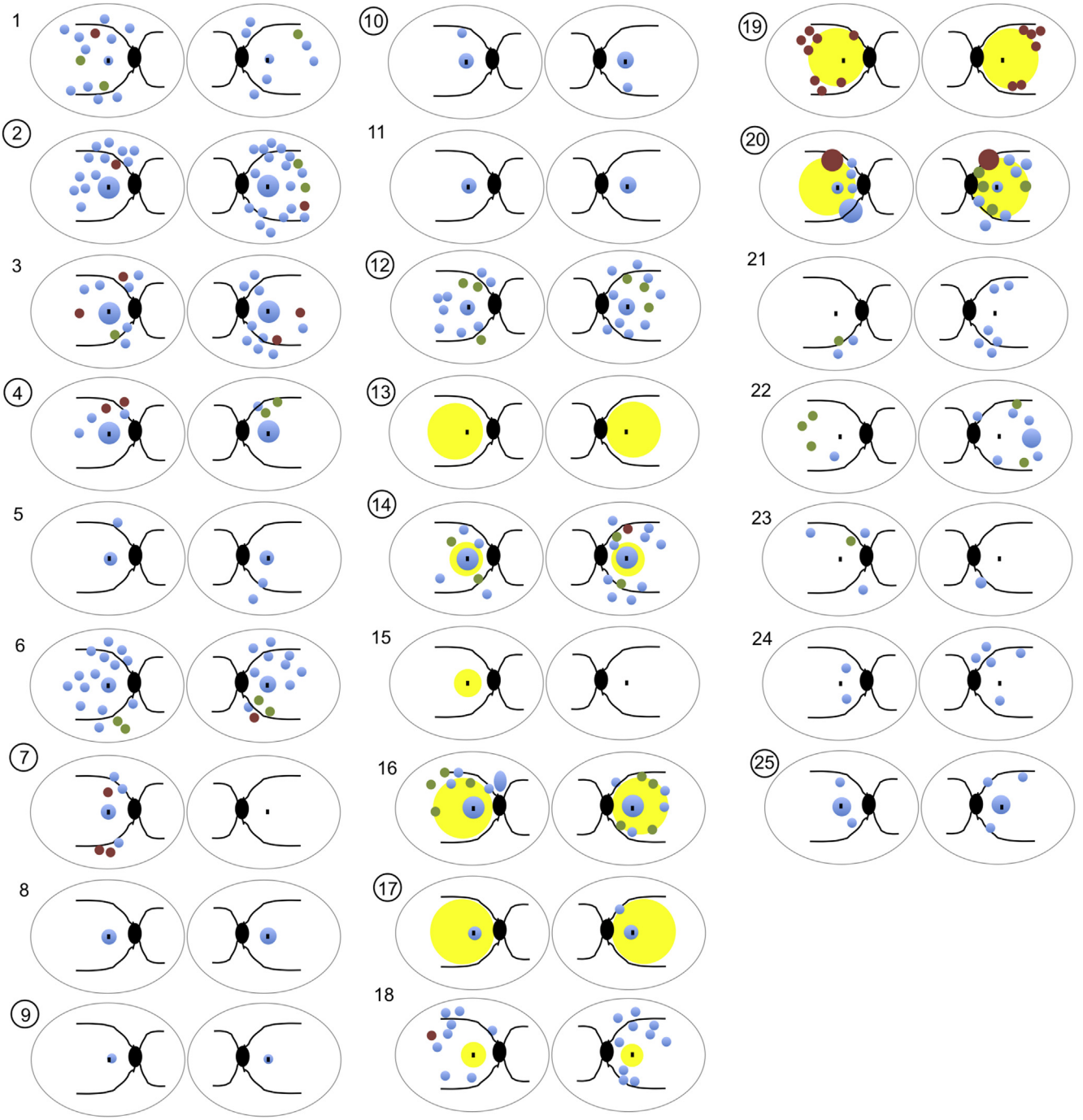

Figure 1. Schematic diagram of 50 eyes of 25 patients showing the location, size, and configuration of each fluid focus: blue = dome, green = caterpillar, red = wavy, yellow = splitting. Number represents patient number and circle designates those patients with visual symptoms. Note the predominantly bilateral, multifocal involvement of the foci and relative symmetry between each eye. Subfoveal fluid foci are dome, if present, and splitting is comparatively widespread. A confluence of fluid foci occurs along the arcades.

wave-like pattern. Splitting (Fig 3, lower) refers to a broad, low-lying accumulation of fluid between the RPE and IZ, the boundaries of which may extend beyond the OCT border. This can be a subtle finding.

These fluid morphologies occurred with the following frequency: of all 313 fluid foci, 231 (73.8%) dome, 36 (11.5%) caterpillar, 31 (9.9%) wavy, and 15 (4.8%) splitting. Except for cases of splitting, the subfoveal fluid focus, if present, had a dome configuration in all eyes.

In all foci, the accumulation of the fluid occurred between the RPE and the IZ (Fig 4). There were neither PEDs nor intraretinal or choroidal hyperreflective dots detected. One eye had concomitant intraretinal cysts, which resolved with subretinal fluid resolution. In 18 of 48 eyes (37.5%), the subfoveal dome-shaped fluid foci

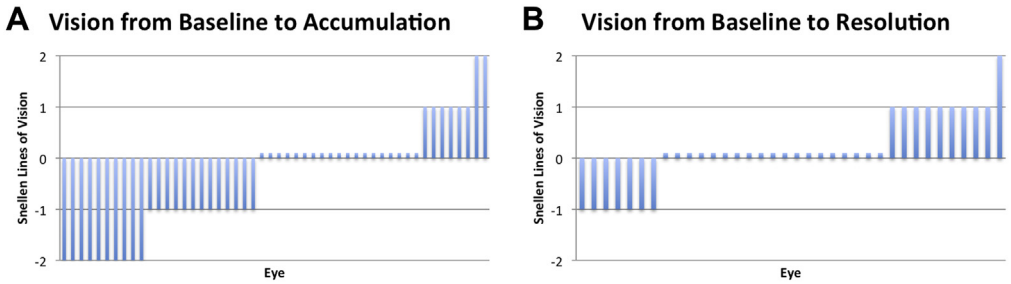

Figure 2. Visual acuity changes at fluid accumulation and resolution. **A**, Waterfall plot demonstrating change in lines of Snellen visual acuity from baseline to fluid accumulation in 49 eyes. **B**, Waterfall plot demonstrating change in lines of Snellen visual acuity from baseline to fluid resolution in 35 eyes. No statistically significant difference was observed between baseline and at fluid resolution, with no greater change of more than 2 Snellen lines.

exhibited elongation of the IZ. In all eyes, the IZ could be distinguished from the RPE and EZ at the time of fluid accumulation; and in 31 of 38 eyes (81.6%), the IZ could *not* be distinguished from the RPE at *baseline*, but became apparent with the accumulation of sub-IZ fluid. In all but 2 foci (99.1%), the RPE, IZ, and EZ layers remained hyperreflective and clearly distinguishable for all fluid foci, both at the time of fluid accumulation and at its resolution. None of the fluid foci were associated with RPE changes at fluid resolution.

Choroidal Thickness

A strong positive interobserver correlation for choroidal thickness measurements was observed ($r = 0.97$, $P < 0.0001$). There was no statistical difference between the mean choroidal thickness at baseline (269.6±15.1 μm) and during fluid accumulation (261.5±15.0 μm) ($P = 0.07$, n = 32 eyes). In addition, there was no statistical difference between the mean choroidal thickness during fluid accumulation (248.1±13.8 μm) and at fluid resolution (247.3±14.0 μm) ($P = 0.99$, n = 31 eyes). Finally, there was no statistical difference between the mean choroidal thickness at baseline (248.2±14.8 μm) and at fluid resolution (247.4±14.9 μm) ($P = 0.97$, n = 29 eyes).

Other Imaging

Fluorescein angiography in 4 eyes revealed no vascular abnormalities, filling defects, blockage, leakage, or staining. Autofluorescence

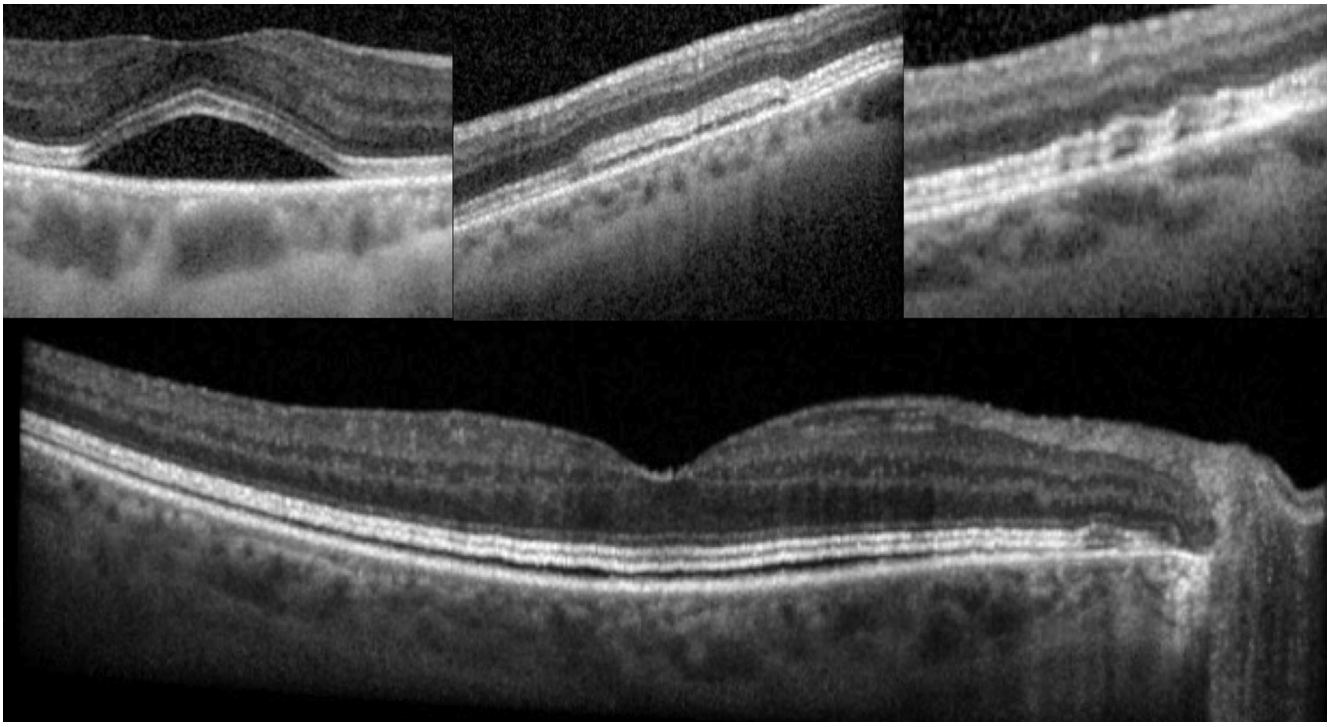

Figure 3. Examples of the 4 fluid configurations. **Upper left**, Domes appear as dome-shaped fluid accumulation between the interdigitation zone (IZ) and retinal pigment epithelium (RPE), akin to the configuration that is observed in classic central serous chorioretinopathy. This larger dome focus displaces both the outer and inner retinal layers. **Upper middle**, Caterpillars appears as a straight or plateaued, low-lying accumulation of fluid, which displaces a portion of the IZ (and outer retinal layers) inward toward the vitreous. **Upper right**, Wavy refers to a linear collection of tiny dome-shaped fluid collections, which displace the IZ (and outer retinal layers) in an undulating, wave-like pattern. **Lower**, Splitting appears as a broad, low-lying accumulation of fluid between the RPE and IZ, the boundaries of which may extend beyond the optical coherence tomography border.

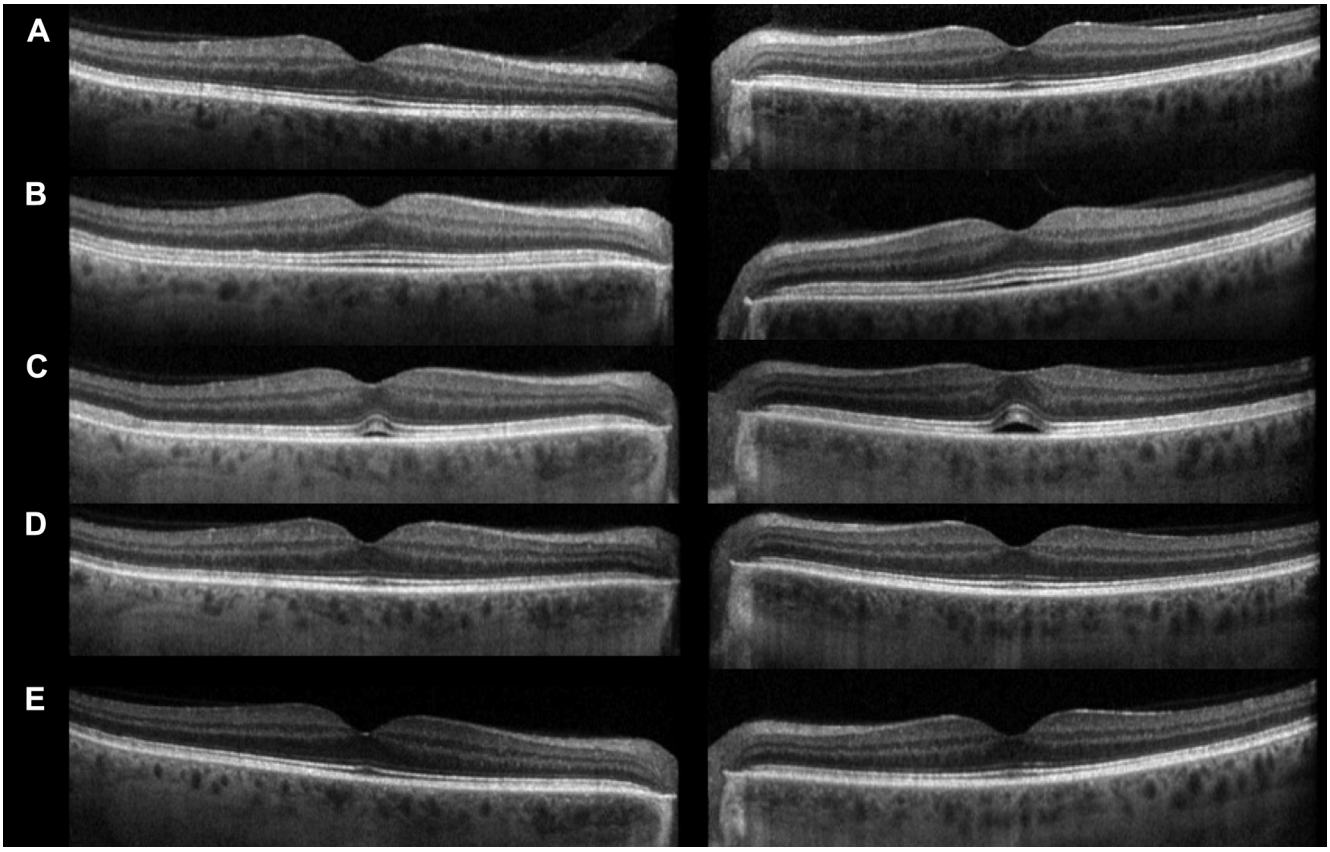

Figure 4. A representative case demonstrating optical coherence tomography findings at baseline, fluid accumulation, and its resolution. Left column = right eye, right column = left eye. **A**, Baseline optical coherence tomography showing normal retinal, retinal pigment epithelium (RPE), and choroidal structures. Note the difficulty in fully distinguishing the interdigitation zone (IZ) from the RPE and ellipsoid zone (EZ). **B**, One day after binimetinib, the IZ shows "splitting" from the underlying RPE. **C**, Ten days after binimetinib, a fluid focus appears in both eyes in a dome configuration (concurrently, multiple foci were present along the superior and inferior arcades—not shown). The IZ is elongated and both the IZ and EZ remain distinguishable and hyperreflective. Note the absence of pigment epithelial detachments, intraretinal edema, and hyperreflective dots. **D**, Forty days after binimetinib, the retinal layers resume their normal appearance and remain so 2 months after drug (**E**). The choroidal thickness remains relatively constant through the fluid evolution.

in 4 eyes was normal, demonstrating no abnormal hyperautofluorescence or hypoautofluorescence.

The comparison of findings between MEKAR and CSC are summarized in Table 2 and Figure 5. An example of CSC in a patient receiving treatment for metastatic melanoma is shown in Figure 6.

Discussion

The MAPK pathway involves a series of activating protein kinases (including MEK), which influence gene transcription and cell proliferation. Dysregulation of this pathway in human cancers makes them susceptible to treatment with targeted drugs that block this pathway, such as MEK inhibitors. For instance, aberrations in the MAPK pathway occur in uveal melanoma and are the premise behind treatment with the MEK inhibitor selumetinib[17]; and MEK inhibition has proven successful in prolonging overall survival of patients with cutaneous melanoma.[18] MEK inhibitors can result in self-limited neurosensory detachments in up to 90% of patients, although many of these patients are asymptomatic.[10]

Some groups have described these neurosensory detachments as being similar to those in CSC.[11,13–15] In fact, the draft of the newest Common Terminology Criteria for Adverse Events (CTCAE version 5.0; available for download at https://ctep.cancer.gov/protocoldevelopment/electronic_applications/…/CTCAEv5.xls; and the standard measure by which oncologists grade toxicity) includes a new entry referring to these foci as either "central serous retinopathy" or "central serous retinal detachment"—evoking a similarity to the well-described clinical disease central serous chorioretinopathy.[19,20] However, other groups acknowledge that the detachments in MEKAR are distinct from those in CSC, and have provided a limited discussion of these differences.[9,10,16]

This study provides an in-depth analysis and demonstrates the clinical and morphologic findings distinguishing MEKAR from CSC. Even in the absence of OCT, MEKAR can be distinguished from CSC purely on the basis of clinical findings. In this study, 92% of patients had simultaneous bilateral foci, which is in contrast to the literature estimate of *up to* 40% of CSC patients with bilateral foci. Furthermore, 77% of patients on MEK inhibition had

Table 2. Summary of Comparisons between MEK Inhibitor–Associated Retinopathy/Pigment and Central Serous Chorioretinopathy

MEKARP	CSC
Bilateral in 92%	Up to 40% bilateral
Multifocal fluid foci (mean 6 foci per eye)	Unifocal or multifocal foci
84% of eyes with subfoveal focus, other foci conglomerate around the arcades	Foci in macula
Fluid foci have four configurations: dome, caterpillar, wavy, or splitting	Fluid focus usually dome configuration
Fluid foci without gravitational dependency: shape of mercury globules	Fluid foci with gravitational dependency and inferior tracking of fluid
Fluid located in sub-IZ: between RPE and IZ	
No RPE detachments or intraretinal/choroidal hyperreflective dots	Majority have RPE detachments or intraretinal/choroidal hyperreflective dots
Elongation of IZ during fluid accumulation (38%)	
During fluid accumulation, IZ distinguishable from EZ and RPE	
Fluid accumulation makes IZ visible in eyes with indistinguishable IZ at baseline	
RPE, IZ, and EZ layers remain hyperreflective and clearly distinguishable, both at the time of fluid accumulation and at its resolution	IZ and EZ can become disturbed and may not reconstitute
Choroidal thickness normal and remains unchanged during fluid accumulation and resolution	Abnormally increased choroidal thickness in diseased and fellow eye
Symptoms include blurry vision, metamorphopsia, dyschromatopsia	Symptoms include blurry vision, metamorphopsia, dyschromatopsia
Majority of patients in this series are female (perhaps reflective of primary cancer diagnosis)	More common in male patients

CSC = central serous chorioretinopathy; EZ = ellipsoid zone; IZ = interdigitation zone; MEKARP = mitogen-activated protein kinase kinase (MEK) inhibitor–associated retinopathy/pigment; RPE = retinal pigment epithelium.

multifocal fluid foci, with a median number of 6 foci per eye. This confirms the findings of other reports that have shown bilateral, multifocal serous elevations typically with subfoveal involvement.[6–8,10–12] Despite only 48% of patients reporting visual symptoms, 83% of eyes in this study had fluid foci involving the fovea.

In this series, the extrafoveal fluid foci mainly accumulate around the arcades (Fig 1), perhaps because of drug accessibility and relative higher concentration around the major blood vessels. Many of the fluid foci in CSC have inferior tracking of fluid (gutter), suggesting a gravitational dependency. In contrast, the MEK inhibitor–associated foci did not exhibit gravitational dependency or inferior fluid tracking, but instead resembled the shape of mercury beads held tight by capillary action. Finally, the number and location of foci appears to be relatively symmetrical between both eyes, perhaps reflective of the systemic drug derivation of fluid accumulation.

At the level of OCT, again, MEKAR is distinct from CSC (Fig 4). In all MEKAR cases, the fluid foci were localized between the RPE and the IZ, an area comprising the apical processes of the RPE and the cone outer segments.[21] Perhaps this distortion of the cone outer segments explains the color perception abnormalities experienced by patients. In normal eyes, the IZ is often indistinguishable from the underlying RPE and overlying EZ on OCT. This was the case in 82% of eyes in this series, which had an indistinguishable IZ at baseline. However, at the time of fluid accumulation, the IZ could be distinguished from both the overlying EZ and underlying RPE in all eyes. Interestingly, the 2 fellow eyes without fluid foci had an absence of photoreceptors and IZ/EZ, presumably from prior damage owing to retinal detachment. In these 2 eyes, the absence of an intact IZ was associated with a lack of fluid accumulation.

Other OCT characteristics commonly found in CSC (PEDs, intraretinal and choroidal hyperreflective dots) were not detected in any of the fluid foci associated with MEK inhibition. The absence of PEDs has been noted in 1 report of 3 cases.[9] In this present series, there was 1 eye with concomitant intraretinal cysts, which resolved with fluid regression. Furthermore, in CSC-fluid foci, a disturbance and loss of, or acquired hyporeflectivity of, the IZ and EZ can be detected on OCT. However, in almost all MEKAR foci (99%), the RPE, IZ, and EZ layers remained hyperreflective and clearly distinguishable, both at the time of fluid accumulation and at its resolution.

Despite this maintenance of hyperreflectivity and eventual resolution of normal anatomy, the IZ can evolve in its appearance during fluid accumulation. In this series of patients with MEK inhibition, just over a third of the fluid foci exhibited elongation of the IZ. Other papers have reported edema of the "outer retinal layers," with specification to "thickening of the retinal pigment epithelium" or the IZ.[6–8] In this study, there was no elongation of the RPE noted and elongation was observed only at the level of the IZ.

The appearance of the fluid foci by OCT could be distinguished into 4 configurations based on the morphology of the sub-IZ fluid and changes to the overlying retinal layers (Fig 3). These configurations include dome, caterpillar, wavy, and splitting and are described in detail in "Results." By far, the most common configuration was dome, followed by caterpillar, wavy, and splitting. It could be hypothesized that these configurations are on a

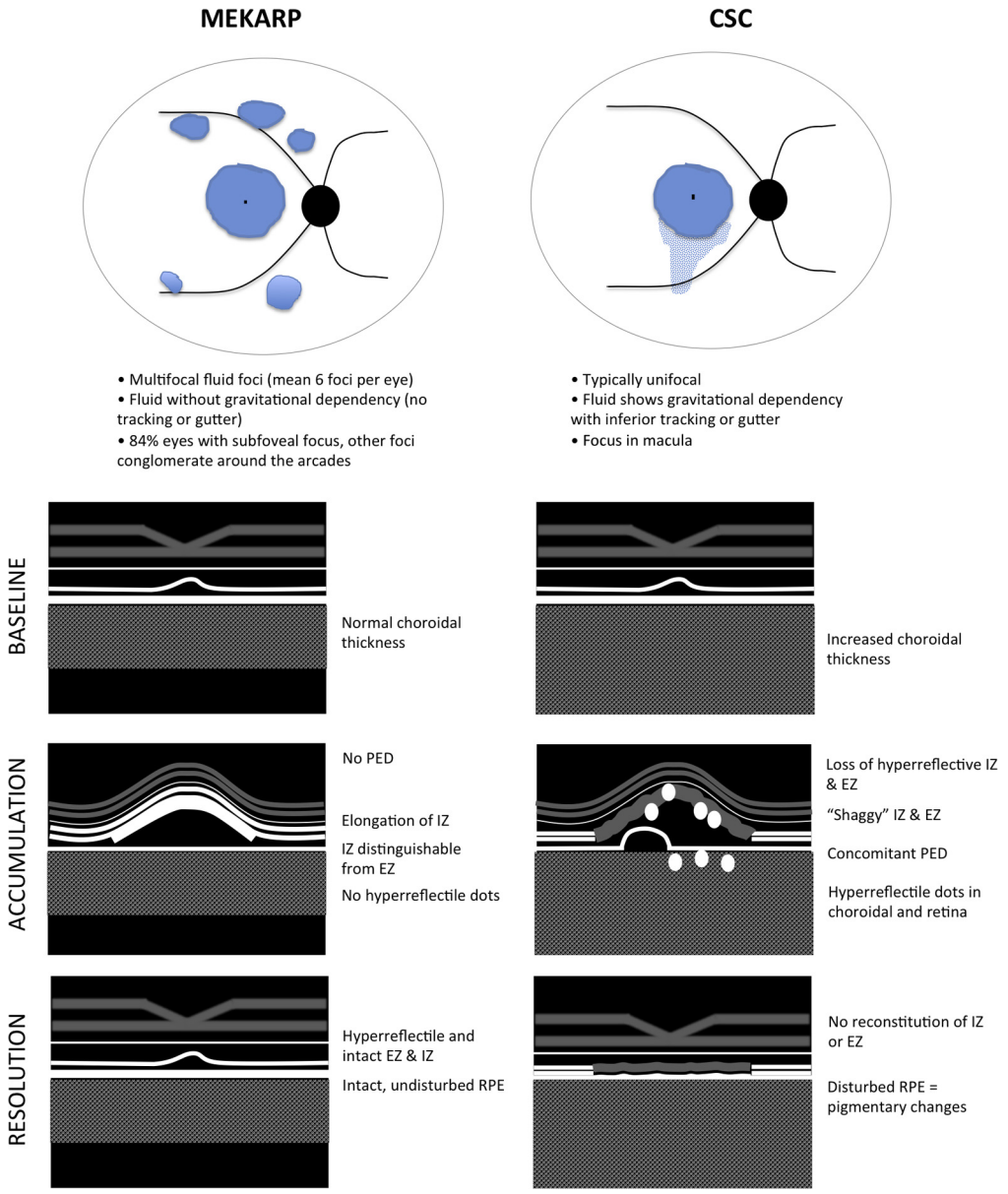

Figure 5. Graphic representation of clinical and morphologic differences in mitogen-activated protein kinase kinase (MEK) inhibitor–associated retinopathy/pigment (MEKAR, *right*) and central serous chorioretinopathy (CSC, *left*). EZ = ellipsoid zone; IZ = interdigitation zone; PED = pigment epithelial detachment; RPE = retinal pigment epithelium.

continuum or represent different stages of fluid accumulation. If this were true, one would expect each focus of fluid to evolve through the 4 stages of configurations. However, this was not observed (although the absence of this observation may be reflective of the prolonged time between examinations). Alternatively, it was apparent that certain configurations are more prone to particular locations in the fundus (Fig 1). For instance, focal subfoveal fluid is "dome" in all cases (except when "splitting" may occur in the absence or presence of the dome), and "wavy" is more typical along the arcades and may represent a confluence of mini-domes. The dome-shaped fluid focus is typical of CSC, but it is unclear if caterpillar, wavy, and splitting configurations occur in this disease.

At some point in their course, MEKAR foci can be yellow in appearance and mimic vitelliform detachments, which are a shared feature with CSC and other retinal diseases. Traditionally, vitelliform foci are predominantly clear at onset, become yellow as they persist, and can even darken as RPE elements and melanosomes seep into the space. Future studies will determine if MEKAR foci assume a similar evolution, although with an intact IZ and RPE and short time to resolution, it is unlikely for them to reach the latter stage (which was not observed in this study). It begs the question whether the location of the fluid (extending

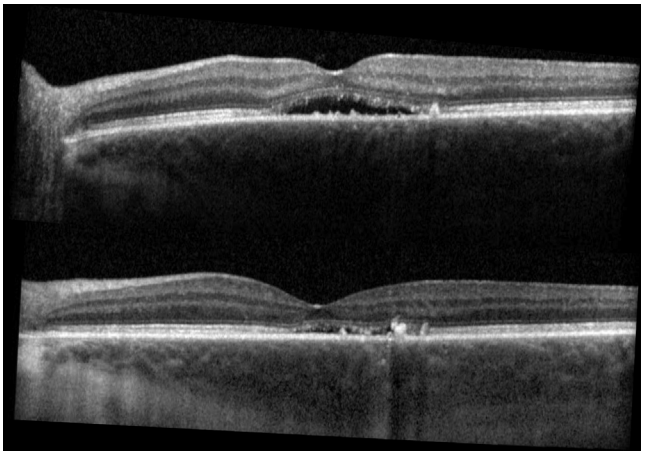

Figure 6. Optical coherence tomography of central serous chorioretinopathy in a patient with metastatic melanoma. This 68-year-old man with metastatic melanoma was receiving systemic prednisone for management of colitis when he reported decreased vision and was found to have subretinal fluid. **Upper,** The optical coherence findings (lack of hyperreflectivity of interdigitation zone [IZ] and ellipsoid zone [EZ], intraretinal and choroid hyperreflective dots, and disturbed retinal pigment epithelium [RPE]) are consistent with central serous chorioretinopathy. **Lower,** At fluid resolution and 20-month follow-up, the IZ/EZ has not reconstituted, and the RPE remains disturbed, as evidenced by pigmentary changes on fundus examination. Also note the relatively thick choroid.

from the RPE to the IZ) is the key feature associated with vitelliform detachments. The relative short duration of fluid in MEKAR likely allows for photoreceptor maintenance and visualization of the fluid in the space bound by the RPE and intact IZ. By contrast, longer-lasting fluid, such as in CSC, has disturbed photoreceptors, which camouflages the precise location of the fluid—presumably also between the RPE and the once intact (but now disturbed) IZ. Further studies will determine if this characteristic is shared by other etiologies of vitelliform detachments and may lead to the adoption of the sub-IZ as the "vitelliform space."

There are a few reported cases of fluorescein angiography and autofluorescence findings in MEK inhibitor–associated serous detachments. The majority of these are consistent with our findings. Specifically, 4 reports established no abnormalities on fluorescein angiography[7,9,10,12] and 2 found normal findings on autofluorescence.[6,7] In 1 case, early hyperfluorescence and late staining of fluid lesions was detected by fluorescein angiography.[8] And in a single other case, hyperautofluorescence was noted by the fluid lesions.[11]

In 2009, it was established that increased choroidal thickness ("pachychoroid"[22]) can be found in both the diseased and fellow eyes of CSC.[23] This pachychoroid may contribute to the pathophysiology of the disease.[24] Others have written on the importance of this discovery in elucidating our understanding of CSC, but lament that "comparable data are not yet available for patients with MEKAR."[16] As such, we investigated whether thickened choroid was a defining feature in MEKAR using comparative measurements of 2 observers with a strong positive interobserver correlation ($r = 0.97$, $P < 0.0001$). We found no statistical difference in the choroidal thickness when comparing measurements at baseline, fluid accumulation, and fluid resolution; and this choroidal thickness was within normal range. This suggests that MEK inhibitor–induced serous detachments may not be associated with a pachychoroid phenotype and that the pathophysiology is exclusive of alterations in choroidal thickness—again, highlighting another distinction between CSC and MEKAR.

A mechanism of fluid accumulation in MEK inhibition has been proposed. Evidence shows that the MAPK pathway regulates tight junctions between RPE cells. Specifically, the MEK pathway can regulate the density of aquaporin 1 (a water-specific transport channel) in RPE cells.[25] However, in this in vitro study of RPE cells, evidence would suggest that MEK inhibition would actually prevent the buildup of fluid. Furthermore, should the defect lie at the level of the RPE, it begs the question why RPE defects or abnormalities are not detected on multimodal imaging (OCT, autofluorescence, fluorescein or indocyanine green angiography), as they are in CSC. For instance, in CSC, 70% to 100% of eyes with acute disease will demonstrate hypoautofluorescence at the leakage point, believed to correspond with a focal RPE defect or RPE cell detachment. Furthermore, 53% to 100% of CSC eyes will have PEDs consistent with a pathophysiology involving abnormal RPE. Present ophthalmic imaging reveals abnormalities at almost a cellular level, but MEK-inhibited eyes may require imaging that detects abnormalities at the *protein* level.

The symptoms of MEKAR are similar to those reported in CSC. Symptoms occurred in 48% of patients, with the most common being blurry vision, but symptoms also included metamorphopsia, or seeing a bubble/doughnut shape or visually sensing an "orange glow" around objects. It is reassuring to patients and their health care team that MEKAR has a mild impact on visual acuity. In this series, no eye lost more than 2 lines of Snellen vision from baseline to fluid accumulation. Furthermore, at the time of fluid resolution, no eye was less than 1 Snellen line from its baseline vision. In all cases, patients maintained vision in a range that allowed them to continue legally driving (in New York State) both at the time of fluid accumulation and at its resolution. It is worth keeping in mind that some patients were examined because of symptoms and some by protocol, limiting our ability to know exactly how many develop the retinal abnormalities in the absence of symptoms. However, it is clear that in this series, MEK inhibitors did not result in irreversible loss of vision or eye damage.

Cancer patients often take many concurrent medications (which may include glucocorticoids), and therefore an understanding of the distinct clinical and morphologic characteristics can distinguish potential steroid-related CSC from subretinal fluid associated with MEK inhibition. Especially since cancer patients with metastatic disease are under stress, by extension, this may have implications on trial drug attribution. MEKAR is predominantly bilateral and multifocal and accumulates in nongravitational rounded globules without fluid tracking or gutter. In contrast to CSC, MEKAR exclusively accumulates in the sub-IZ space, often revealing this space in eyes with an IZ

indistinguishable from the RPE at baseline. The IZ can temporarily elongate, but unlike cases of CSC, the IZ and EZ remain intact and hyperreflective during fluid accumulation and its resolution. The fluid foci can assume 4 distinct configurations. Unique from CSC, the RPE and choroid remain normal during MEK inhibition and its associated subretinal fluid. These findings would benefit from confirmation by a prospective study in a larger cohort with short-interval repeat imaging.

References

1. Akinleye A, Furqan M, Mukhi N, et al. MEK and the inhibitors: from bench to bedside. *J Hematol Oncol*. 2013;6:27.
2. Fouladi M, Stewart CF, Blaney SM, et al. A molecular biology and phase II trial of lapatinib in children with refractory CNS malignancies: a pediatric brain tumor consortium study. *J Neurooncol*. 2013;114:173-179.
3. Turner MC, Rossfeld K, Salama AKS, et al. Can binimetinib, encorafenib and masitinib be more efficacious than currently available mutation-based targeted therapies for melanoma treatment? *Expert Opin Pharmacother*. 2017;18:487-495.
4. Dummer R, Schadendorf D, Ascierto PA, et al. Binimetinib versus dacarbazine in patients with advanced NRAS-mutant melanoma (NEMO): a multicentre, open-label, randomised, phase 3 trial. *Lancet Oncol*. 2017;18:435-445.
5. Liu CY, Francis JH, Brodie SE, et al. Retinal toxicities of cancer therapy drugs: biologics, small molecule inhibitors, and chemotherapies. *Retina*. 2014;34:1261-1280.
6. Urner-Bloch U, Urner M, Jaberg-Bentele N, et al. MEK inhibitor-associated retinopathy (MEKAR) in metastatic melanoma: long-term ophthalmic effects. *Eur J Cancer*. 2016;65:130-138.
7. Urner-Bloch U, Urner M, Stieger P, et al. Transient MEK inhibitor-associated retinopathy in metastatic melanoma. *Ann Oncol*. 2014;25:1437-1441.
8. Duncan KE, Chang LY, Patronas M. MEK inhibitors: a new class of chemotherapeutic agents with ocular toxicity. *Eye (Lond)*. 2015;29:1003-1012.
9. McCannel TA, Chmielowski B, Finn RS, et al. Bilateral subfoveal neurosensory retinal detachment associated with MEK inhibitor use for metastatic cancer. *JAMA Ophthalmol*. 2014;132:1005-1009.
10. Weber ML, Liang MC, Flaherty KT, Heier JS. Subretinal fluid associated with MEK inhibitor use in the treatment of systemic cancer. *JAMA Ophthalmol*. 2016;134:855-862.
11. Schoenberger SD, Kim SJ. Bilateral multifocal central serous-like chorioretinopathy due to MEK inhibition for metastatic cutaneous melanoma. *Case Rep Ophthalmol Med*. 2013;2013:673796.
12. Niro A, Strippoli S, Alessio G, et al. Ocular toxicity in metastatic melanoma patients treated with mitogen-activated protein kinase kinase inhibitors: a case series. *Am J Ophthalmol*. 2015;160(5):959-967.e1.
13. Velez-Montoya R, Olson J, Petrash M, et al. Acute onset central serous retinopathy with MEK inhibitor use for metastatic cancer. *Invest Ophthalmol Vis Sci*. 2011:E—abstract 2153.
14. Purbrick RMJ, Osunkunle OA, Talbot DC, Downes SM. Ocular toxicity of mitogen-activated protein kinase inhibitors. *JAMA Oncol*. doi:10.1001/jamaoncol.2016.4213.
15. Maubon L, Hirji N, Petrarca R, Ursell P. MEK inhibitors: a new class of chemotherapeutic agents with ocular toxicity. *Eye (Lond)*. 2016;30:330.
16. Montana CL, Apte RS. MEKanisms of a serous complication. *JAMA Ophthalmol*. 2017;135(5):413-414.
17. Carvajal RD, Sosman JA, Quevedo JF, et al. Effect of selumetinib vs chemotherapy on progression-free survival in uveal melanoma: a randomized clinical trial. *JAMA*. 2014;311:2397-2405.
18. Long GV, Stroyakovskiy D, Gogas H, et al. Combined BRAF and MEK inhibition versus BRAF inhibition alone in melanoma. *N Engl J Med*. 2014;371:1877-1888.
19. Yannuzzi LA. Central serous chorioretinopathy: a personal perspective. *Am J Ophthalmol*. 2010;149:361-363.
20. Yannuzzi LA. Type-A behavior and central serous chorioretinopathy. *Retina*. 1987;7:111-131.
21. Staurenghi G, Sadda S, Chakravarthy U, et al. Proposed lexicon for anatomic landmarks in normal posterior segment spectral-domain optical coherence tomography: the IN•OCT consensus. *Ophthalmology*. 2014:1572-1578.
22. Dansingani KK, Balaratnasingam C, Klufas MA, et al. Optical coherence tomography angiography of shallow irregular pigment epithelial detachments in pachychoroid spectrum disease. *Am J Ophthalmol*. 2015;160:1243-1254.e2.
23. Imamura Y, Fujiwara T, Margolis R, Spaide RF. Enhanced depth imaging optical coherence tomography of the choroid in central serous chorioretinopathy. *Retina*. 2009;29:1469-1473.
24. Yang L, Jonas JB, Wei W. Optical coherence tomography-assisted enhanced depth imaging of central serous chorioretinopathy. *Invest Ophthalmol Vis Sci*. 2013;54:4659-4665.
25. Jiang Q, Cao C, Lu S, et al. MEK/ERK pathway mediates UVB-induced AQP1 downregulation and water permeability impairment in human retinal pigment epithelial cells. *Int J Mol Med*. 2009;23:771-777.

Footnotes and Financial Disclosures

Originally received: April 30, 2017.
Final revision: May 30, 2017.
Accepted: May 31, 2017.
Available online: July 12, 2017. Manuscript no. 2017-1003.

[1] Ophthalmic Oncology Service, Memorial Sloan Kettering Cancer Center, New York, New York.

[2] Weill-Cornell Medical Center, New York, New York.

[3] Vitreous, Retina, Macula Consultants of New York, New York, New York.

[4] The LuEsther T. Mertz Retina Research Laboratory, New York, New York.

[5] Department of Medicine, Gynecologic Medical Oncology Service, Memorial Sloan Kettering Cancer Center, New York, New York.

[6] Department of Medicine, Memorial Sloan Kettering Cancer Center, New York, New York.

[7] Human Oncology and Pathogenesis Program, Memorial Sloan Kettering Cancer Center, New York, New York.

Financial Disclosure(s):
The authors made the following disclosures: M.P.: Advisory board — Array BioPharma and Novartis.

N.H.S.: Consulting and research funds — Roche/Genentech, MedImmune/AstraZeneca, and Pfizer.

P.B.C.: Support – Merck, Genentech, Daiichi Sankyo, Genentech, Provectus, Bio Connections LLC, IMS Health, Haymarket Media, Roche; Grants – Pfizer, BMS; Payment for development of educational presentations – Medscape.

Supported by the Fund for Ophthalmic Knowledge, The New York Community Trust, Research to Prevent Blindness, Geoffrey Beene Cancer Research Center at Memorial Sloan Kettering Cancer Center, and Cancer Center Support Grant (P30 CA008748). The sponsor or funding organization had no role in the design or conduct of this research.

Author Contributions:

Conception and design: Francis

Analysis and interpretation: Francis, Habib, Abramson, Yannuzzi, Catalanotti

Data collection: Francis, Habib, Heinemann, Gounder, Grisham, Postow, Shoushtari, Chi, Segal, Yaeger, Ho, Chapman, Catalanotti

Obtained funding: Not applicable

Overall responsibility: Francis, Habib, Abramson, Yannuzzi, Heinemann, Gounder, Grisham, Postow, Shoushtari, Chi, Segal, Yaeger, Ho, Chapman, Catalanotti

Abbreviations and Acronyms:
BCVA = best-corrected visual acuity; **CSC** = central serous chorioretinopathy; **CSR** = central serous retinopathy; **EZ** = ellipsoid zone; **IZ** = interdigitation zone; **MAPK** = mitogen-activated protein kinase; **MEK** = mitogen-activated protein kinase kinase; **MEKAR** = MEK inhibitor–associated retinopathy; **OCT** = optical coherence tomography; **PED** = pigment epithelial detachment; **RPE** = retinal pigment epithelium.

Correspondence:
Jasmine H. Francis, MD, FACS, Memorial Sloan Kettering Cancer Center, 1275 York Ave, New York, NY 10065. E-mail: francij1@mskcc.org.

Pictures & Perspectives

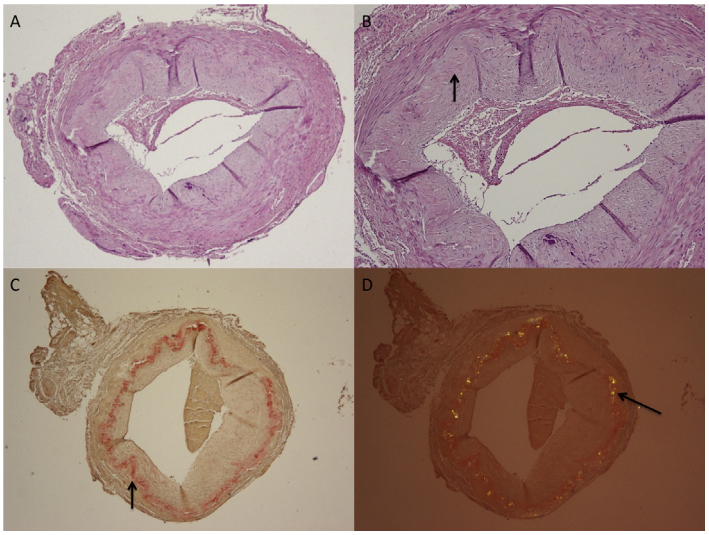

Amyloidosis Mimicking Temporal Arteritis in Multiple Myeloma

A 77-year-old man with a recent diagnosis of kappa light chain IgA multiple myeloma presented with amaurosis fugax of the left eye, jaw claudication, and arthritis. Erythrocyte sedimentation rate (ESR) was 11 and C-Reactive Protein (CRP) was 2. The patient underwent subsequent left temporal artery biopsy. Examination by light microscopy revealed an amorphous, hypocellular, eosinophilic staining material infiltrating the internal elastic lamina (Fig 1**A** and **B**, *arrow*) (hematoxylin and eosin, magnification 40× and 100×, respectively). There were no signs of an inflammatory infiltrate. Congo red staining confirmed the presence of amyloid (Fig 1**C**, *arrow*, magnification 40×) with characteristic apple-green birefringence under cross-polarized light (Fig 1**D**, *arrow*, magnification 40×). (Magnified version of Fig 1**A-D** is available online at www.aaojournal.org).

Gregory D. Kramer, MD[1,2]
Dorota Lebiedz-Odrobina, MD[3]
Nick Mamalis, MD[1]

[1]Department of Ophthalmology and Visual Sciences, John A. Moran Eye Center, University of Utah, Salt Lake City, Utah; [2]Department of Ophthalmology, Nassau University Medical Center, East Meadow, New York; [3]Division of Rheumatology, University of Utah, Salt Lake City, Utah